Chemical Physics Letters 627 (2015) 77–81

Contents lists available at ScienceDirect

Chemical Physics Letters

journal homepage: www.elsevier.com/locate/cplett

The non-ideal behaviour of the interfacial tension of the *n*-heptane + perfluoro-*n*-hexane mixture: A computational study

Hector Dominguez

Instituto de Investigaciones en Materiales, Universidad Nacional Autónoma de México, UNAM, México, D.F. 04510, Mexico

ARTICLE INFO

Article history:
Received 27 December 2014
In final form 19 March 2015
Available online 30 March 2015

ABSTRACT

Computer simulations of the *n*-heptane + perfluoro-*n*-hexane system is used to understand the unusual behaviour of the horizontal inflection of the vapour–liquid interfacial tension experiments of alkanes–perfluoroalkanes mixtures. Simulations are conducted and good agreement with experiments is obtained. From the results a change in curvature to a nearly constant value in the tensions at high perfluoro-*n*-hexane compositions is identified. Dynamic, thermodynamic and structural properties are analysed in that region and peculiar tendencies of those properties are found which help us to understand the nature of the uncommon inflection in the isotherms.

1. Introduction

It is well known that mixtures of alkanes–perfluoroalkanes present a different behaviour from the ideal; for instance, the large positive deviation from Raoult's law, the large positive excess functions and the liquid–liquid immiscibility [1,2]. In particular, the vapour–liquid interface tension presents a horizontal inflection close to the critical composition which has been observed in actual experiments [3,4] and predicted by the square gradient theory of van der Waals [5,6]. In fact, those studies have suggested that the anomalous behaviour could be due to the unusually weak attractive interaction between the alkane and perfluoroalkane molecules [7–11]. From the experimental point of view alkane + perfluoroalkane mixtures have been studied in previous works [12,13] whereas from the theoretical point of view, a successful approach to investigate those mixtures has been the statistical associating fluids theory (SAFT) which has proved to be a reliable method in the study of these systems [2,14–20].

On the other hand, computer simulations have also proved to be a powerful technique to study alkanes–perfluoroalkanes systems [21–23]. For instance the interfacial tension of the *n*-heptane + perfluoro-*n*-hexane ($C_6F_{14} + C_7H_{16}$) system was simulated in a previous work and the results shown good agreement with SAFT data and with experiments [24]. The principal interest of that previous work was the construction of a computational model to reproduce the experiments such as the liquid–liquid equilibria and the interfacial tension. The model was also validated with an equation of state (SAFT). In the present letter that computational model is used to obtain more information and to better understand how properties change along the interfacial tension, before and after the inflection. Then, molecular dynamics simulations are carried out to study, from a molecular point of view, the interfacial tension isotherms of the *n*-heptane + perfluoro-*n*-hexane mixture. In particular we investigate few structural, thermodynamic and dynamic properties to better understand the nature of the interfacial tension in the system.

2. Model

As it was mentioned above the computational model is the same used in our anterior work [24], i.e. the binary mixture is simulated with the molecular dynamics methodology using the same force field reported in previous letters [24–28]. The force field includes inter- and intra-molecular interactions. The intramolecular interactions have harmonic bonds, harmonic angles and dihedral potentials whereas the inter-molecular interactions consider Lennard-Jones potentials with parameters taken from earlier works [25–28]. In order to handle correctly the deviations, in the *n*-heptane + perfluoro-*n*-hexane mixture, from the ideal behaviour the cross interactions, given in the Berthelot rule, are corrected in the Lennard-Jones potential [24,29]

$$\epsilon_{ij} = (1 - \kappa_{ij})\sqrt{\epsilon_{ii}\epsilon_{jj}} \tag{1}$$

where ϵ_{ii} is the well depth of the Lennard-Jones potential. For the present simulations it was used $\kappa_{ij} = 0.1$ since that value reproduced correctly the liquid–liquid equilibria of the mixture [24].

E-mail address: hectordc@unam.mx

http://dx.doi.org/10.1016/j.cplett.2015.03.039
0009-2614/

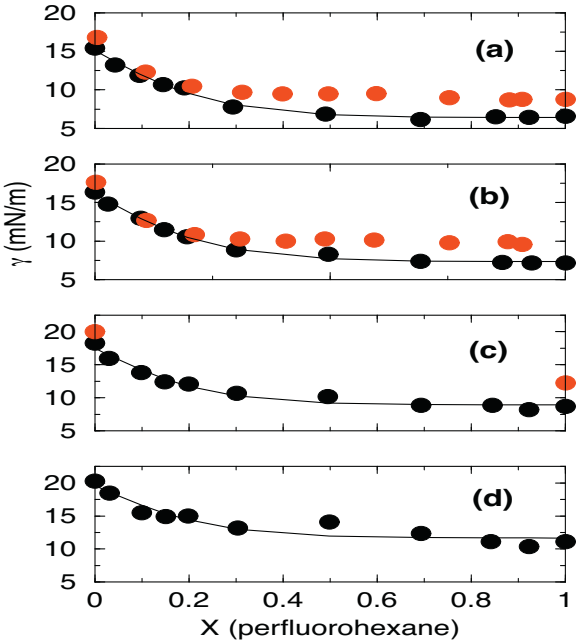

Figure 1. The interfacial tensions (γ) of the vapour–liquid interface of the *n*-heptane + perfluoro-*n*-hexane at (a) $T = 328.15$ K, (b) $T = 318.15$ K, (c) $T = 298.15$ K and (d) $T = 273.15$ K. The red circles are experimental data taken from Ref. [3] and the black circles are the computer simulations of the present work. The solid lines are the fitted functions explained in the text. (For interpretation of the references to colour in this figure legend, the reader is referred to the web version of the article.)

All simulations were run with the DL-POLY package [30] in the NVT ensemble, using the Hoover-Nosé thermostat [31] with a relaxation time of 0.1 ps and a time step of 0.005 ps. The initial configurations were prepared with *n*-heptane and perfluoro-*n*-hexane molecules located randomly in the middle of a rectangular box, with a vapour–liquid interface, of dimensions $X = Y = 43.0$ Åand $Z = 300$ Å. The number of *n*-heptane and perfluoro-*n*-hexane molecules was chosen in order to have several compositions in the mixture (with a total of 980 molecules). The usual periodic boundary conditions in all three directions were used and the Lennard-Jones interactions were cut off at 15 Å. Finally, several temperatures were simulated up to 20 ns using the last 5 ns for data analysis.

3. Results

3.1. Interfacial tension

In Figure 1 the vapour–liquid interfacial tensions are calculated and plotted at different temperatures, $T = 273.15$, 298.15, 318.15 and 328.15 K, as a function of the perfluoro-*n*-hexane composition, x_p. Those temperatures correspond to temperatures below, close to, and above the experimental critical point. The interfacial tension is obtained by the mechanical approach by calculating the components of the pressure tensor [32]. At low perfluoro-*n*-hexane compositions the interfacial tensions are in good agreement with the experiments whereas at high compositions the simulation results slightly deviate from them, nevertheless, they reflect qualitatively a similar trend with respect to the actual experiments.

It is worthy to mention that the present simulations were run at the same conditions of those reported in our previous work [24] and it is observed that the isotherms do not change significantly, i.e. data are in agreement with previous results. In fact, from the isotherms, it is possible to depict an inflection around the perfluoro-*n*-hexane composition of $x_p \approx 0.2$. Then, the curves show nearly a constant

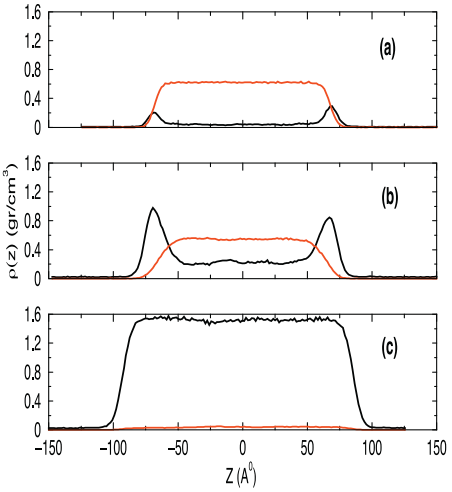

Figure 2. Density profiles, $\rho(z)$, of the *n*-heptane + perfluoro-*n*-hexane mixture at $T = 318.15$ K at different perfluoro-*n*-hexane compositions. (a) $x_p = 0.04$, (b) $x_p = 0.2$ and (c) $x_p = 0.9$. Black and red solid lines represent the perfluoro-*n*-hexane and the *n*-heptane profiles, respectively. (For interpretation of the references to colour in this figure legend, the reader is referred to the web version of the article.)

behaviour at high compositions. It is important to say that close to the same composition ($x_p \approx 0.2$) it is also reported an inflection in the vapour–liquid composition curves (see Refs. [13,24]).

In order to estimate where the isotherms present a constant value, in our simulation data, the curves are fitted with the function $\gamma = A_0(\tanh(A_1 x_p)) + A_2$ (where A_0, A_1 and A_2 are fitted parameters) for all the data and with a straight line only for the last points. Then, the composition where the isotherms reach nearly a constant behaviour can be estimated as the intersection of both fitted curves. In all cases that composition is around $x_p \approx 0.7$. In fact, that value is close to the composition where a second inflection in the vapour–liquid equilibria curves is observed in previous simulations and experimental works [13,24]. Therefore, a region between compositions (0.2–0.7) is identified where the interfacial tension presents a change in curvature.

3.2. Structure

The first analysis is conducted in terms of density profiles for the different perfluoro-*n*-hexane compositions. Since all profiles present similar features only representatives graphs, at temperature $T = 318.15$ K, are shown in Figure 2. At low compositions it is observed that perfluoro-*n*-hexane molecules are adsorbed mostly at the vapour–liquid interface with few molecules uniformly distributed in the bulk liquid mixture. As the perfluoro-*n*-hexane composition increases there is an increment of those molecules at the interface indicated by the high peaks in the profiles (see Figure 2b). From composition $x_p \approx 0.2$ and up to composition $x_p \approx 0.7$ the perfluoro-*n*-hexanes do not present regular distributions in the liquid–liquid phase. Moreover, there are regions where an excess of perfluoro-*n*-hexane molecules are observed in comparison with *n*-heptane molecules. Longer simulations were run, from composition $x_p \approx 0.2$ to $x_p \approx 0.7$ (up to 30 ns), however, the same trends are observed. However, from composition $x_p \approx 0.8$ both perfluoro-*n*-hexane and *n*-heptane present a regular distribution along the mixture as noted in Figure 2c.

The structure of the chains is also analysed by an order parameter,

$$S_{zz} = \frac{1}{2}\langle 3\cos^2\theta - 1\rangle \qquad (2)$$

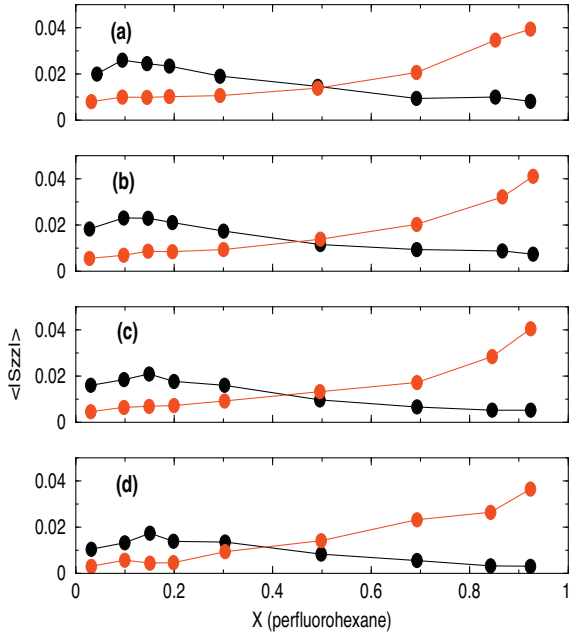

Figure 3. The average order parameter, $\langle|S_{zz}|\rangle$, of the CH_n and CF_n groups of *n*-heptane + perfluoro-*n*-hexane mixture at different temperatures and perfluoro-*n*-hexane compositions. Black circles are for perfluoro-*n*-hexane and red circles for *n*-heptane. (a) $T = 328.15$ K, (b) $T = 318.15$ K, (c) $T = 298.15$ K and (d) $T = 273.15$ K. The solid lines are included as a guide for the eye. (For interpretation of the references to colour in this figure legend, the reader is referred to the web version of the article.)

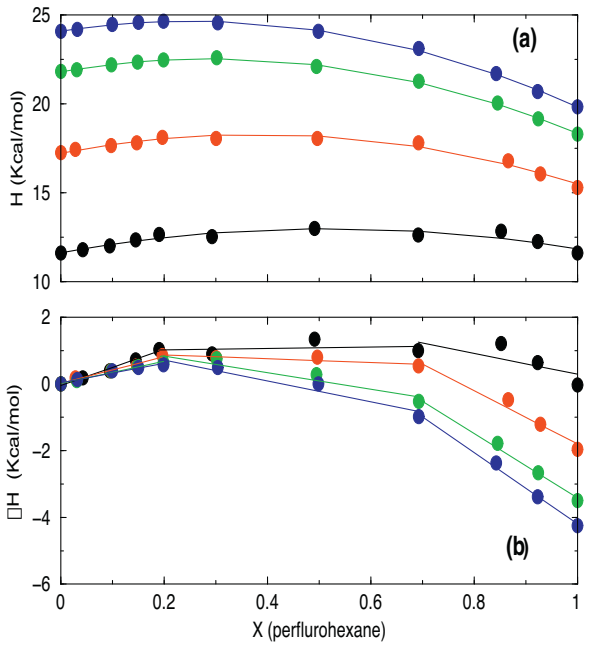

Figure 4. Enthalpies (a) and change in enthalpy (b) of the *n*-heptane + perfluoro-*n*-hexane mixture for different temperatures and perfluoro-*n*-hexane compositions. Blue data for $T = 328.15$ K, green data for $T = 318.15$ K, red data for $T = 298.15$ K and black data for $T = 273.15$ K. The continuous solid lines in panel (a) are the fitted curves to the data. The solid lines in panel (b) are linear functions fitted to the data. (For interpretation of the references to colour in this figure legend, the reader is referred to the web version of the article.)

where θ is the angle between the vector normal to the interface and the vectors which joint nearest neighbour atoms along the chain. For $S_{zz} = -0.5$ the molecules present a complete order parallel to the interface and for $S_{zz} = 1.0$ the order is normal to the interface.

In Figure 3, the order parameter $\langle|S_{zz}|\rangle$ averaged over all the CH_n and CF_n groups (in vapour and liquid phases) in *n*-heptane and perfluoro-*n*-hexane molecules, respectively, is plotted. Despite the small values it is possible to observe a tendency in the plots. In fact, at low perfluoro-*n*-hexane compositions ($<x_p = 0.2$) the CF_n groups (black data) present higher order than the CH_n groups (red data). As the number of perfluoro-*n*-hexane molecules increases the order of the CH_n groups increases while the order of the CF_n groups decreases. Moreover, above composition $x_p = 0.4$ a crossover in the order parameter is observed and the order of the alkanes becomes higher than that of the perfluoroalkanes. Furthermore, from composition $x_p = 0.7$, where the constant behaviour of the interfacial tension starts, the $\langle|S_{zz}|\rangle$ of *n*-heptane has a significant increment with respect to the $\langle|S_{zz}|\rangle$ of perfluoro-*n*-hexane. Since the cross interaction of *n*-heptane with perfluoro-*n*-hexane is weaker than the interaction between molecules of the same specie (due to the partial miscibility) it seems that at low compositions the perfluoroalkane chains do not feel much attraction with the other alkane molecules. Therefore, the structure of the few perfluoro-*n*-hexane molecules is not modified significantly and it could be the reason of the higher order of those molecules with respect to the order of the alkanes. Similar arguments could be used at low *n*-heptane compositions, in that case the order is reversed, i.e. the order of the alkane chains is higher than that of the perfluoroalkane chains. The same trend is observed for all the temperatures studied (see Figure 3).

3.3. Enthalpy

Enthalpies of the systems are also calculated and plotted in Figure 4. Even though the small differences in the enthalpies it is possible to depict a maximum value which can be estimated by fitting a quadratic curve over the data. The errors associated to the data are of the size of the symbols. The maximum enthalpies are located at compositions $x_p = 0.25$, 0.29, 0.38 and 0.52 for temperatures $T = 328.15$, 318.15, 298.15 and 273.15, respectively (see Figure 4a), i.e. between the composition region of (0.2 and 0.7). In fact, it is observed that the maximum enthalpy is shifted to high compositions as the temperature is reduced. On the other hand, the change in enthalpy, $\Delta H = H - H_0$ (where H_0 is the enthalpy at composition zero), is also evaluated and plotted in Figure 4b. In that plot data are fitted with a straight line in three different regions; region 1 from composition $x_p = 0.0$ to $x_p = 0.2$; region 2 from composition $x_p = 0.2$ to $x_p = 0.7$ and region 3, from composition $x_p = 0.7$ to $x_p = 1.0$. Then, it is observed how the slopes of the straight lines dramatically change in each region, around $x_p = 0.2$ and $x_p = 0.7$ which are the compositions where the curvature is defined in the interfacial tension.

3.4. Diffusion coefficient

An extra analysis is calculated for a dynamical property, the self diffusion coefficient of the CH_n and CF_n groups in the mixture (Figure 5). In this case the diffusion coefficients are evaluated by calculating the mean square displacements of the CH_n and CF_n groups. Moreover, the diffusion is calculated over all CF_n and CH_n groups in the perfluoro-*n*-hexane and *n*-heptane molecules, i.e. in the liquid and vapour phases. At low perfluoro-*n*-hexane compositions there are few of those molecules at the vapour–liquid interface which have low mobility, however, there are also molecules in the vapour phase with high mobility, i.e. they have high diffusion coefficients. Our own simulations of a pure perfluoro-*n*-hexane system at very low densities (vapour phase) give even higher diffusion coefficients than those obtained in Figure 5. Then, the diffusion coefficients plotted in Figure 5 are the contribution of all molecules in both phases which could explain the high diffusion

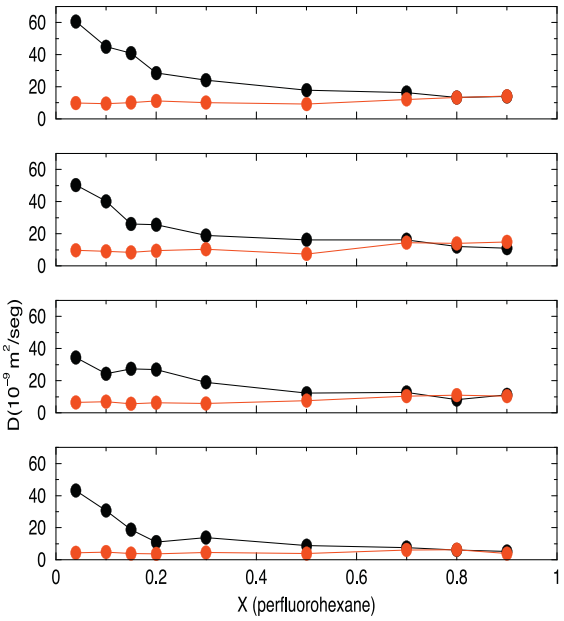

Figure 5. Diffusion coefficients of the *n*-heptane + perfluoro-*n*-hexane mixture for different temperatures and perfluoro-*n*-hexane compositions. Black circles are for perfluoro-*n*-hexane and red circles for *n*-heptane. The solid lines are included as a guide for the eye. (a) $T = 328.15$ K, (b) $T = 318.15$ K, (c) $T = 298.15$ K and (d) $T = 273.15$ K. (For interpretation of the references to colour in this figure legend, the reader is referred to the web version of the article.)

of the perfluoro-*n*-hexane at low compositions. As the perfluoro-*n*-hexane composition increases there are more molecules in the bulk liquid than in the vapour region. Therefore, in this case, the main contribution in the diffusion comes from those molecules in the liquid and the total diffusion coefficient diminishes. On the other hand, since only few *n*-heptane molecules are in the vapour phase the diffusion coefficient for this specie is given by the molecules in the liquid region. Therefore, the diffusion coefficient of the alkanes does not change significantly as shown in Figure 5. As a general trend, it is observed that the diffusion coefficient of perfluoro-*n*-hexane is higher than that of the *n*-heptane. However, as the perfluoro-*n*-hexane composition increases the diffusion of CF_n decreases whereas the diffusion of CH_n does not change significantly. In fact, from composition $x_p \approx 0.7$ the diffusion coefficients of both components have similar values as observed in Figure 5. The experimental bulk diffusion coefficient of heptane, at $T = 298$ K, is about 3×10^9 m^2/seg [33] which is smaller than the value found in the present work at zero perfluoro-*n*-hexane composition ($\approx 8 \times 10^9$ m^2/seg). In the case of the perfluoro-*n*-hexane a bulk diffusion coefficient of 4×10^9 m^2/seg is reported at temperature $T = 298$ K [34] whereas a value of $\approx 11 \times 10^9$ m^2/seg, at the same temperature, is found in the present work. However, diffusions in the present letter, as mentioned above, are calculated in the vapour–liquid system (not in bulk) and it could be the reason of the difference with the reported values.

4. Conclusions

Dynamical computer simulations are used to understand the inflection of the interfacial tension of the *n*-heptane + perfluoro-*n*-hexane binary mixture. Even though the simulation data present a slightly deviation from the experiments at high compositions, they give us a good overall description and behaviour of the vapour–liquid interfacial tension and the general shape of the curves [3].

In the present work the partial miscibility is represented by the weaker interaction of the different alkanes–perfluoroalkanes molecules. In fact, due to the immiscibility of the mixture the physical properties present different behaviour in the region where the isotherms have a change in curvature. From the force field we have that the CH_n–CH_n interactions are stronger than the CF_n–CF_n and the cross interactions. Therefore, at low perfluoro-*n*-hexane compositions those molecules, at the interface, do not present strong forces with the rest of the *n*-heptane molecules and it could be reason why they remain at the vapour–liquid interface as indicated in the density profiles. As the number of perfluoro-*n*-hexane molecules increases those molecules are more distributed in the system and then, less adsorption at the interface is observed.

From the surface tension plots it is observed that the curvature changes faster at low perfluoro-*n*-hexane compositions (up to $x_p \approx 0.2$) with a negative slope. By analysing the density profiles and the order parameter ($\langle |S_{zz}| \rangle$) we note structure differences at those low compositions. It seems that the variations become from the perfluoro-*n*-hexane molecules since those molecules are mainly adsorbed at the interface and they present higher order than the *n*-heptane molecules.

At rich perfluoro-*n*-hexane compositions the order of those molecules is lower than that of the *n*-heptanes. Moreover, at high perfluoro-*n*-hexane compositions (low alkane compositions) the *n*-heptane is not adsorbed at the interface, i.e. there is not evidence of any excess of those molecules at the interface since it is not observed any alkane peaks in the density profiles at the vapour–liquid interface. Therefore, the results suggest that the inflection in the isotherms could be due to lose of structure and order at the interface. On the other hand, the reduction in the structure and order are also followed by a change in enthalpy since a variation of that quantity is observed in the same regions where the isotherms present a change in curvature.

Finally, the present results give us new insights to explain the interfacial tension of the vapour–liquid interface in the mixture. Moreover, since there are other alkanes-perfluoroalkanes mixtures which exhibit a similar non-ideal tendency [3] they might have an analogous behaviour of the properties analysed in the present *n*-heptane + perfluoro-*n*-hexane system.

Acknowledgements

The author acknowledges support from Grants DGAPA-UNAM-Mexico IN102812, CONACyT-Mexico 154899 and DGTIC-UNAM for the supercomputer facilities. The author would like to thank the reviewers for their valuable comments to improve the manuscript.

References

[1] L. Lepori, E. Matteoli, A. Spanedda, C. Duce, M.R. Tine, Fluid Phase Equilib. 20 (2002) 119.
[2] P. Morgado, C. McCabe, E.J.M. Filipe, Fluid Phase Equilib. 228 (2005) 389.
[3] I.A. McLure, R. Whitfield, J. Bowers, J. Colloid Interface Sci. 203 (1998) 31.
[4] I.A. McLure, B. Edmonds, M. Lal, Nat. Phys. Sci. 241 (1973) 71.
[5] B. Widom, J. Chem. Phys. 67 (1977) 872.
[6] F.F. Ramos Gomez, B. Widom, Physica A 104A (1980) 595.
[7] J.H. Hildebrand, B.B. Fisher, H.A. Benesi, J. Am. Chem. Soc. 72 (1950) 4348.
[8] J.B. Hickman, J. Am. Chem. Soc. 77 (1955) 6154.
[9] J.H. Simons, J.W. Mausteller, J. Chem. Phys. 20 (1952) 1516.
[10] T.M. Reed, J. Phys. Chem. 63 (1959) 1798.
[11] J.S. Rowlinson, F.L. Swinton, Liquids and Liquid Mixtures, 3rd edn., Butterworth scientific, London, 1982.
[12] C. Duce, M.R. Tine, L. Lepori, E. Matteoli, Fluid Phase Equilib. 199 (2002) 197.
[13] R.A. Khairulin, S.V. Stankus, V.A. Gruzdev, V.A. Bityutskii, Russ. J. Phys. Chem. A 83 (2009) 50.
[14] C. McCabe, A. Galindo, A. Gil-Villegas, G. Jackson, J. Phys. Chem. B 102 (1998) 8060.
[15] E.J.M. Filipe, E.J.S. Gomez de Azevedo, L.F.G. Martins, V.A.M. Soares, J.C.G. Calado, C. McCabe, G. Jackson, J. Phys. Chem. B 104 (2000) 1315.
[16] E.J.M. Filipe, L.M.B. Dias, J.C.G. Calado, C. McCabe, G. Jackson, Phys. Chem. Chem. Phys. 4 (2002) 1618.
[17] L.M.B. Dias, R.P. Bonifacio, E.J.M. Filipe, J.C.G. Calado, C. McCabe, G. Jackson, Fluid Phase Equilib. 205 (2003) 163.

[18] A.M.A. Dias, J.C. Pamies, J.A.P. Coutinho, I.M. Marrucho, L.F. Vega, J. Phys. Chem. B 108 (2004) 1450.
[19] M.J. Pratas de Melo, A.M.A. Dias, M. Blesic, L.P.N. Rebelo, L.F. Vega, J.A.P. Coutinho, I.M. Marrucho, Fluid Phase Equilib. 242 (2006) 210.
[20] M.C. dos Ramos, F. Blas, Mol. Phys. 10 (2010) 1349.
[21] W. Song, P.J. Rossky, M. Maroncelli, J. Chem. Phys. 119 (2003) 9145.
[22] L. Zhang, J.I. Siepmann, J. Phys. Chem. B 109 (2005) 2911.
[23] J.J. Potoff, D.A. Bernard-Brunel, J. Phys. Chem. B 113 (2009) 14725.
[24] H. Dominguez, A.J. Haslam, G. Jackson, E.A. Müller, J. Mol. Liq. 185 (2013) 36.
[25] L. Zhang, J.I. Siepmann, J. Phys. Chem. B 109 (2005) 2911.
[26] S.K. Nath, F.A. Escobedo, J.J. de Pablo, J. Chem. Phys. 108 (1998) 9905.
[27] W.L. Jorgensen, J.D. Madura, C.J. Swenson, J. Am. Chem. Soc. 106 (1984) 6638.
[28] S.T. Cui, J.I. Siepmann, H.D. Cochran, P.T. Cummings, Fluid Phase Equilib. 146 (1998) 51.
[29] A.J. Haslam, A. Galindo, G. Jackson, Fluid Phase Equilib. 266 (2008) 105.
[30] T.R. Forester, W. Smith, DL-POLY Package of Molecular Simulation, CCLRC, Daresbury Laboratory, Daresbury, Warrington, England, 1996.
[31] M.P. Allen, D.J. Tildesley, Computer Simulation of Liquids, Clarendon Press, Oxford, 1993.
[32] J.S. Rowlinson, B. Widom, Molecular Theory of Capillarity, Clarendon, Oxford, 1982.
[33] J.W. Moore, R.M. Wellek, J. Chem. Eng. Data 19 (1974) 138.
[34] C. McCabe, D. Bedrov, O. Borodin, G.D. Smith, P.T. Cummings, Ind. Eng. Chem. Res. 42 (2003) 6956.